Neurobiology of Disease 180 (2023) 106070

Contents lists available at ScienceDirect

Neurobiology of Disease

journal homepage: www.elsevier.com/locate/ynbdi

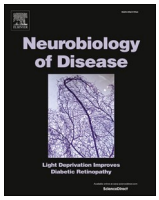

MRI-based basal forebrain atrophy and volumetric signatures associated with limbic TDP-43 compared to Alzheimer's disease pathology

Stefan Teipel [a,b,*], Michel J. Grothe [c], The Alzheimer's Disease Neuroimaging Initiative [1]

[a] Deutsches Zentrum für Neurodegenerative Erkrankungen (DZNE) Rostock/Greifswald, Rostock, Germany
[b] Department of Psychosomatic Medicine, Rostock University Medical Center, Rostock, Germany
[c] Unidad de Trastornos del Movimiento, Servicio de Neurología y Neurofisiología Clínica, Instituto de Biomedicina de Sevilla, Hospital Universitario Virgen del Rocío/CSIC/Universidad de Sevilla, Seville, Spain

ARTICLE INFO

Keywords:
Limbic TDP-43
Cholinergic deficit
MRI
Autopsy
AD pathology
Imaging signature

ABSTRACT

Background: It is not clear to which degree limbic TDP-43 pathology associates with a cholinergic deficit in the absence of Alzheimer's disease (AD) pathology.
Objective: Replicate and extend recent evidence on cholinergic basal forebrain atrophy in limbic TDP-43 and evaluate MRI based patterns of atrophy as a surrogate marker for TDP-43.
Methods: We studied ante-mortem MRI data of 11 autopsy cases with limbic TDP-43 pathology, 47 cases with AD pathology, and 26 mixed AD/TDP-43 cases from the ADNI autopsy sample, and 17 TDP-43, 170 AD, and 58 mixed AD/TDP-43 cases from the NACC autopsy sample. Group differences in basal forebrain and other brain volumes of interest were assessed using Bayesian ANCOVA. We assessed the diagnostic utility of MRI based patterns of brain atrophy using voxel-based receiver operating characteristics and random forest analyses.
Results: In the NACC sample, we found moderate evidence for the absence of a difference in basal forebrain volumes between AD, TDP-43, and mixed pathologies (Bayes factor$(BF)_{10} = 0.324$), and very strong evidence for lower hippocampus volume in TDP-43 and mixed cases compared with AD cases ($BF_{10} = 156.1$). The ratio of temporal to hippocampus volume reached an AUC of 75% for separating pure TDP-43 from pure AD cases. Random-forest analysis between TDP-43, AD, and mixed pathology reached only a multiclass AUC of 0.63 based on hippocampus, middle-inferior temporal gyrus, and amygdala volumes. Findings in the ADNI sample were consistent with these results.
Conclusion: A comparable degree of basal forebrain atrophy in pure TDP-43 cases compared to AD cases encourages studies on the effect of cholinergic treatment in amnestic dementia due to TDP-43. A distinct pattern of temporo-limbic brain atrophy may serve as a surrogate marker to enrich samples in clinical trials for the presence of TDP-43 pathology.

1. Introduction

TAR DNA-binding protein 43 (TDP-43) in the medial temporal lobe and limbic system is a frequent co-pathology in Alzheimer's disease (AD) (Josephs et al., 2014; Josephs et al., 2008; Robinson et al., 2018), but is also found in older people with amnestic dementia without concurrent AD changes (Katsumata et al., 2020). The latter has been categorized as limbic-predominant age-related TDP-43 encephalopathy (LATE) (Nelson et al., 2019). In a previous study, we used volumetric analysis of ante-mortem MRI (Kilimann et al., 2014) from the autopsy cohort of the Alzheimer's Disease Neuroimaging Initiative (ADNI) to assess atrophy of the cholinergic basal forebrain in limbic TDP-43-only cases compared to AD-only cases (Teipel et al., 2022). We had found that the two groups did not differ in the degree of basal forebrain atrophy, suggesting a similar cholinergic deficit in both pathological conditions.

Here, we replicated and extended the previous findings in an independent autopsy sample from the National Alzheimer Coordinating Center (NACC) cohort (Morris et al., 2006). We now also included cases

* Corresponding author at: Department of Psychosomatic Medicine, University of Rostock, and DZNE Rostock, Gehlsheimer Str. 20, 18147 Rostock, Germany.
E-mail address: stefan.teipel@med.uni-rostock.de (S. Teipel).

[1] Part of the data used in preparation of this article were obtained from the Alzheimer's Disease Neuroimaging Initiative (ADNI) database (adni.loni.usc.edu/). As such, the investigators within the ADNI contributed to the design and implementation of ADNI and/or provided data but did not participate in analysis or writing of this report. A complete listing of ADNI investigators can be found at: http://adni.loni.usc.edu/wp-content/uploads/how_to_apply/ADNI_Acknowledgement_List.pdf

https://doi.org/10.1016/j.nbd.2023.106070
Received 4 January 2023; Received in revised form 23 February 2023; Accepted 5 March 2023
Available online 8 March 2023

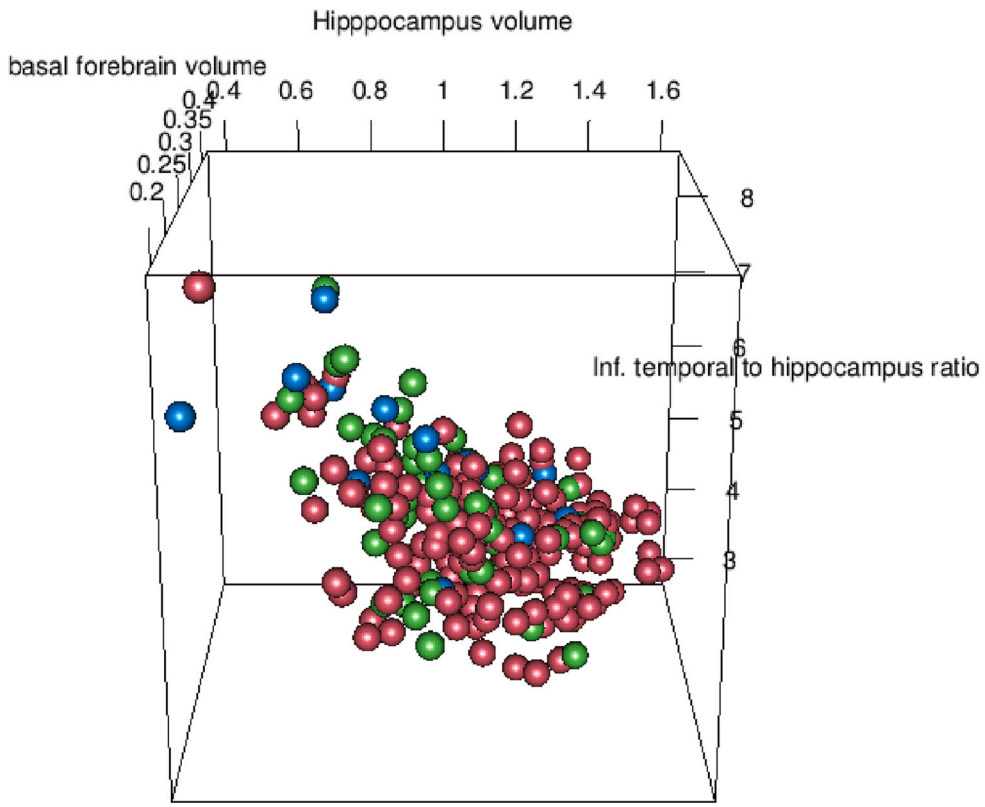

Fig. 1. Distribution of key volumes across pure AD, pure TDP-43 and mixed AD/TDP-43 cases.
3D plot of hippocampus and basal forebrain volume, and inferior-middle temporal gyrus to hippocampus ratio labeled according to group membership (red - AD, green - mixed cases, blue - TDP-43) from the NACC data.

with mixed AD/TDP-43 pathology in addition to individuals with pure AD or pure TDP-43 pathology from the ADNI and the NACC cohorts. We hypothesized that the extent of basal forebrain atrophy would not differ between pure TDP-43 and pure AD cases, but that mixed pathology would be associated with more pronounced atrophy than TDP-43 pathology alone. Finally, we investigated the diagnostic utility of volumetric MRI markers for TDP-43 pathology. Currently, there is no validated molecular biomarker for TDP-43 pathology in the brain; for example, experimental CSF-derived markers are not yet ready for use in clinical research (Scialo et al., 2020). In this situation, an MRI-based surrogate marker for TDP-43 pathology could be useful to include or exclude individuals with a higher likelihood of limbic TDP-43 pathology from a clinical trial. Results from two FDG-PET studies and one MRI study suggest that hippocampal and middle-inferior temporal lobe regions may be useful, if not for identifying individual cases, at least at the group level (Botha et al., 2018; Grothe et al., 2022; Teipel et al., 2022). We tested these regional markers in the ADNI and the NACC autopsy samples and compared their performance with the diagnostic power of a data-driven volumetric signature identified through cross-validated voxel-wise ROC analysis and a random forest classifier model, which also allows for non-linear group separation.

2. Material and methods

2.1. Data source

Data used in the preparation of this article were obtained from two databases, the ADNI database (http://adni.loni.usc.edu/) and the National Alzheimer's Coordinating Center (NACC) database (https://naccdata.org). The ADNI was launched in 2003 by the National Institute on Aging, the National Institute of Biomedical Imaging and Bioengineering, the Food and Drug Administration, private pharmaceutical companies and non-profit organizations, with the primary goal of testing whether neuroimaging, neuropsychological, and other biologic measurements can be used as reliable in-vivo markers of AD pathogenesis. A fuller description of ADNI and up-to-date information is available at www.adni-info.org. NACC data are collected since 2005 during standardized annual evaluations conducted at the NIA-funded Alzheimer's Disease Research Centers (ADRCs) across the US.

All procedures performed in the ADNI and NACC studies involving human participants were in accordance with the ethical standards of the institutional research committees and with the 1964 Helsinki declaration and its later amendments. Written informed consent was obtained from all participants and/or authorized representatives and the study partners before any protocol-specific procedures were carried out in the ADNI and NACC studies.

2.2. Study participants

We retrieved the last available MRI scans of 100 ADNI subjects who had come to autopsy between 2007 and 2022. In addition we retrieved 188 autopsy cases from the NACC cohort with available MRI scans. For both cohorts, we used the last available clinical dementia rating (CDR) global score (Morris, 1993) for categorization into different severities of cognitive impairment: Healthy controls with a CDR global score of 0, mild cognitive impairment with a CDR global score of 0.5, and dementia with a CDR score of 1 or larger.

2.3. Neuropsychological testing

The CDR global and sum of boxes scores (CDR-SB) were available for all cases. Since 2005, the NACC cohort has collected the so called Uniform Data Set (UDS) of cognitive tests. The first and second version of the UDS (Weintraub et al., 2009) included the mini mental state

Table 1
Demographics of ADNI autopsy sample.

	AD group (n = 47)	TDP-43 group (n = 11)	mixed group (n = 26)
Last clinical diagnosis* (HC, MCI, ADD, missing)[1]	1/9/37/0	0/4/6/1	0/2/24/0
Sex (female/male)[2]	12/35	2/9	6/20
Age at death (mean, 95% CI) [years][3]	81.9 (79.8–84.1)	86.6 (82.5–90.7)	84.0 (81.2–86.9)
Distance between MRI and death (mean, 95% CI) [years][4]	2.9 (2.1–3.6)	3.2 (0.8–5.5)	4.1 (2.9–5.2)
Basal forebrain neuron loss[5] (none/mild/moderate/severe/missing)**	1/23/1/0/22	0/5/0/0/6	0/13/0/13
Hippopcampal sclerosis (no/yes)[6]	47/0	7/4	21/5
Lewy body pathology[7] (no/brainstem/limbic/neocortical/amygdala/olfactory bulb)	22/2/2/10/11/0	4/2/1/4/0/0	13/0/4/5/2/2

* Clinical diagnosis is based on last available CDR global scores.
** Since the question was on an effect of TDP43 compared with AD pathology on number of neurons in the basal forebrain, we did not include mixed cases in this analysis.
[1] Bayes factor shows no conclusive evidence for a dependency between pathological groups and clinical diagnoses (BF_{10}) = 0.873; i.e., a dependency between pathological groups and clinical diagnoses is 1/0.873 = 1.2 times less likely than the independence of both factors.
[2] Bayes factor in favor of no dependency; BF_{10} = 0.089.
[3] Bayes factor shows no conclusive evidence; BF_{10} = 0.656.
[4] Bayes factor shows no conclusive evidence (BF_{10}) = 0.441.
[5] Bayes factor shows no conclusive evidence (BF_{10}) = 0.367; pairwise comparison of pure AD and pure TDP-43 cases with a BF_{10} = 0.388.
[6] Bayes factor shows very strong evidence in favor of a difference, BF_{10} = 385.2.
[7] Bayes factor shows no conclusive evidence (BF_{10}) = 0.715.

Table 2
Demographics of NACC autopsy sample.

	AD group (n = 170)	TDP-43 group (n = 17)	mixed group (n = 58)
Last clinical diagnosis* (HC, MCI, ADD)[1]	8/22/140	0/2/15	0/5/53
Sex (female/male)[2]	84/86	5/12	28/30
Age at death (mean, 95% CI) [years][3]	80.1 (78.5–81.6)	84.6 (79.1–90.2)	84.1 (81.9–86.4)
Distance between MRI and death (mean, 95% CI) [years][4]	5.5 (5.0–5.9)	6.8 (4.8–8.7)	6.9 (6.0–7.7)
Hippopcampal sclerosis (no/yes/missing)[5]	154/11/5	9/8/0	44/13/1
Lewy body pathology[6] (no/brainstem/limbic/cortical/unspecified/missing)	87/6/45/28/3/1	11/0/2/4/0/0	28/0/17/12/1/0

* Clinical diagnosis is based on last available CDR global scores.
[1] Bayes factor shows strong evidence against a difference between groups, BF_{10} = 0.036.
[2] Bayes factor shows strong evidence against a difference between groups; BF_{10} = 0.071.
[3] Bayes factor shows moderate evidence for a difference between groups, BF_{10} = 3.841, with moderate evidence for a difference between pure AD and mixed AD-TDP cases (BF_{10} = 4.422), and inconclusive evidence for the other group comparisons in post hoc tests.
[4] Bayes factor shows moderate evidence for a difference between groups, BF10 = 8.657, with strong evidence for a difference between pure AD and mixed AD-TDP cases (BF10 = 13.238), and inconclusive evidence for the other group comparisons in post hoc tests.
[5] Bayes factor shows extreme evidence in favor of a difference, BF_{10} = 5035.
[6] Bayes factor shows extreme evidence in favor of no difference, BF_{10} = $1.8*10^{-4}$.

Table 3
Post hoc tests for hippocampus and middle-inferior temporal gyrus to hippocampus ratio volumes across pure AD, pure TDP-43, and mixed AD/TDP-43 cases in the ADNI cohort.

Hippocampus volume

Group vs.	Group	Prior odds	Posterior odds	$BF_{10, U}$
AD	TDP-43	0.587	0.760	1.293
	AD/TDP-43	0.587	0.670	1.141
TDP-43	AD/TDP-43	0.587	0.241	0.410

Middle-inferior temporal gyrus to hippocampus ratio

Group vs.	Group	Prior odds	Posterior odds	$BF_{10, U}$
AD	TDP-43	0.587	101.731	173.188
	AD/TDP-43	0.587	3.104	5.284
TDP-43	AD/TDP-43	0.587	0.360	0.613

The posterior odds have been corrected for multiple testing by fixing to 0.5 the prior probability that the null hypothesis holds across all comparisons (Westfall et al., 1997). Individual comparisons are based on the default t-test with a Cauchy (0, r = 1/sqrt(2)) prior. The "U" in the Bayes factor denotes that it is uncorrected.

Table 4
Post hoc tests for hippocampus and middle-inferior temporal gyrus to hippocampus ratio volumes across pure AD, pure TDP-43, and mixed AD/TDP-43 cases in the NACC cohort.

Hippocampus volume

Group vs.	Group	Prior odds	Posterior odds	$BF_{10, U}$
AD	TDP-43	0.587	10.084	17.167
	AD/TDP-43	0.587	12.279	20.904
TDP-43	AD/TDP-43	0.587	0.292	0.497

Middle-inferior temporal gyrus to hippocampus ratio

Group vs.	Group	Prior odds	Posterior odds	$BF_{10, U}$
AD	TDP-43	0.587	658.990	1121.873
	AD/TDP-43	0.587	28.272	48.131
TDP-43	AD/TDP-43	0.587	0.592	1.009

The posterior odds have been corrected for multiple testing by fixing to 0.5 the prior probability that the null hypothesis holds across all comparisons (Westfall et al., 1997). Individual comparisons are based on the default t-test with a Cauchy (0, r = 1/sqrt(2)) prior. The "U" in the Bayes factor denotes that it is uncorrected.

examination (MMSE), a range of tests of memory (including logical memory), attention (including digit span), verbal fluency, naming (Boston naming), and psychomotor speed and cognitive flexibility (trail making test (TMT) A and B). In contrast to the CDR, the UDS cognitive tests were only available in a minority of cases for the last visit before death. For analyses, we used MMSE score, logical memory, digit span forward, and TMT-B minus TMT-A (TMTB-A), which were available on average only in about 40 cases from the AD group, 4 to 6 cases from the TDP-43 group, and 14 to 16 cases from the mixed AD/TDP-43 group.

2.4. Neuropathological assessments

All neuropathological evaluations in the ADNI cohort are performed through the central laboratory of the ADNI neuropathology core (http://adni.loni.usc.edu/about/#core-container) (Franklin et al., 2015). NACC autopsy evaluations are conducted at each of the participating AD research centers. The neuropathological procedures in ADNI and NACC follow previously established guidelines (Montine et al., 2012) that are captured in the format of the NACC Neuropathology Data Form Version 10 (https://www.alz.washington.edu/NONMEMBER/

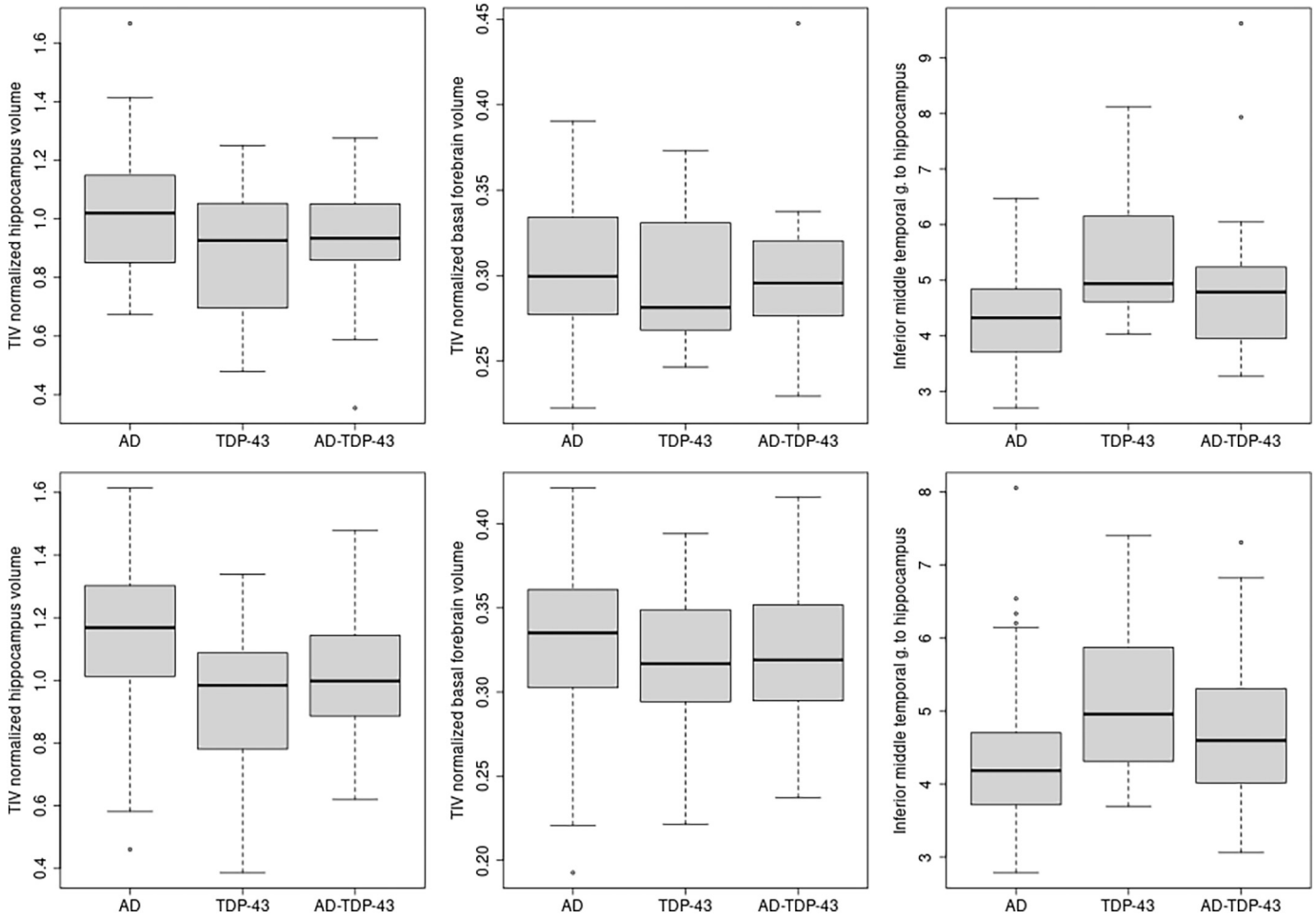

Fig. 2. Boxplots of volumes by TDP-43 status.
a: ADNI.
b: NACC.

Table 5
Spatial clusters reaching a voxel-wise AUC of 80% or higher in the training sample.

Centroid MNI coordinates (x/y/z)	Voxel per cluster	Anatomical region of centroid	Addit. anatomical regions covered by the cluster
−27/−72/33	108	Left superior occipitalis gyrus	–
45/38/−15	113	Right inferior frontal gyrus	Right middle frontal gyrus
−39/−87/−9	176	Left inferior occipital gyrus	–
60/−35/−20	189	Right inferior temporal gyrus	Right fusiform gyrus
33/−86/12	206	Right middle occipital gyrus	–
48/−68/15	533	Right middle temporal gyrus	Right middle occipital gyrus
−42/−81/15	613	Left middle occipital gyrus	Left middle temporal gyrus
32/−47/−21	1178	Right fusiform gyrus	Right cerebellum, anterior lobe
−62/−30/−12	3183	Left middle temporal gyrus	Left fusiform gyrus, inferior temporal gyrus, superior temporal gyrus

Anatomical regions were derived using the "Tailarach Daemon" implemented in FSLeyes and by visual inspection of the Talairach atlas itself (Talairach and Tournoux, 1988).

NP/npform10.pdf), as described in (Besser et al., 2018).

Here, we applied established rating scales for the presence of TDP-43 pathology and AD pathology, respectively. Cases were classified as relatively pure TDP-43 if they had TDP-43 pathology in at least two of the following four regions: amygdala, hippocampus, entorhinal/inferior temporal cortex or neocortex (TDP-43 sum score 2 or higher), and an NIA-AA Alzheimer's disease neuropathologic change (ADNC) score below 2, indicating no or low presence of AD pathology. By contrast, cases were classified as pure AD if they had an ADNC score of 2 or higher, indicating at least moderate presence of AD pathology, and a TDP-43 sum score of 0, indicating no TDP-43 pathology in any of the four regions. Cases were classified as mixed pathology if the TDP-43 sum score was $\geq$2 and the ADNC score was $\geq$2. Presence of hippocampal sclerosis was assessed, and Lewy body pathology was rated following the NACC Neuropathology Data Form. In the ADNI autopsy cohort semi-quantitative ratings of Nucleus basalis Meynert neuronal loss (none, mild, moderate, and severe) were available in a subset of cases. Such rating was not available for the NACC sample.

2.5. *Imaging data acquisition*

Detailed acquisition and standardized pre-processing steps of ADNI imaging data are available at the ADNI website (https://adni.loni.usc.edu/methods/). Structural MRI scans were acquired on multiple 1.5 T and 3 T MRI scanners using scanner-specific T1-weighted sagittal 3D MPRAGE sequences. MRI scans undergo standardized preprocessing

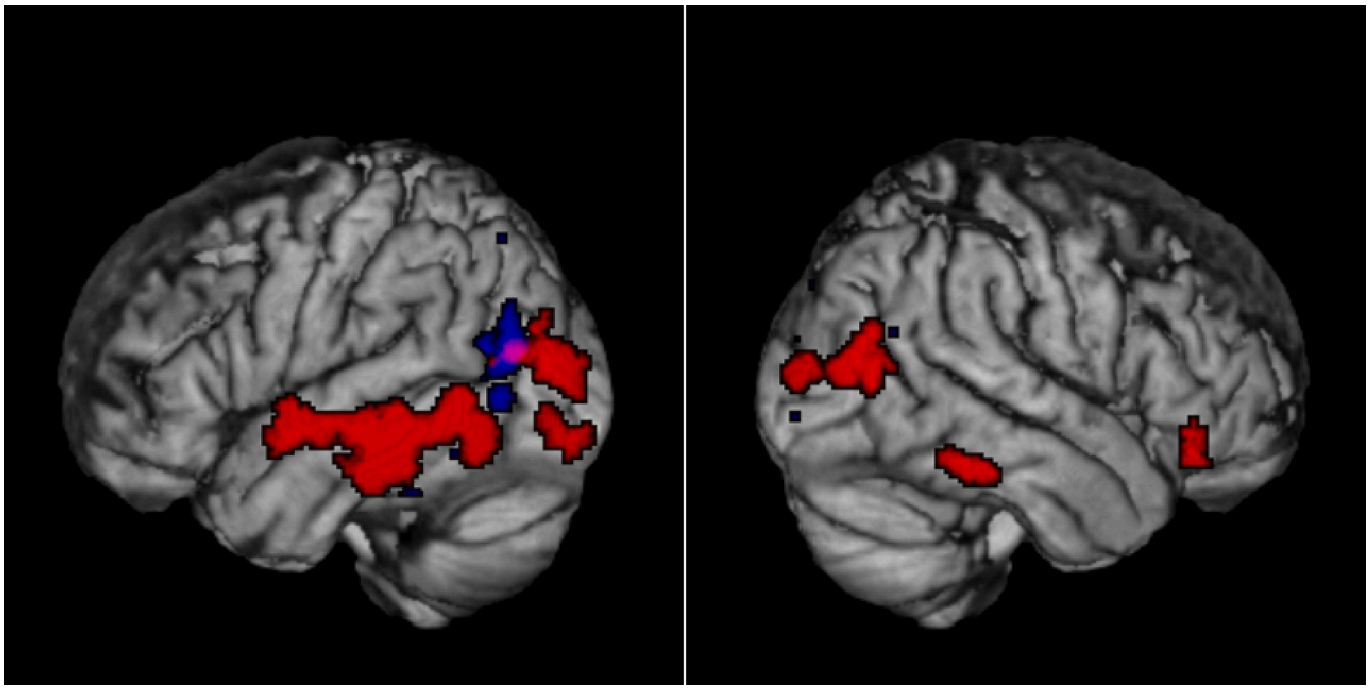

Fig. 3. Clusters discriminating pure AD and pure TDP-43 cases in the ADNI and NACC samples.
Red: Clusters with a voxel-wise AUC of 80% or higher discriminating pure AD and pure TDP-43 cases in the ADNI sample projected onto a rendered surface projection in MNI standard space. Blue: Clusters with a voxel-wise AUC of 70% or higher discriminating pure AD and pure TDP-43 cases in the NACC sample. Pink: Spatial overlap between the ADNI and the NACC clusters.

steps aimed at increasing data uniformity across the multicenter scanner platforms (see https://adni.loni.usc.edu/methods/ for detailed information on multicentric MRI acquisition and preprocessing in ADNI). MR imaging data from NACC represent a convenience sample, voluntarily submitted by several Alzheimer's Disease Research Centers. They include data from multiple 1.5 and 3.0 Tesla scanners without a priori harmonization of sequences. We only retrieved volumetric MRI scans using scanner-specific T1-weighted sequences.

2.6. Imaging data pre-processing

Images were preprocessed using Statistical Parametric Mapping software version 12 (SPM12) (The Wellcome Trust Centre for Neuroimaging, Institute of Neurology, University College London) implemented in Matlab 2019. MRI images were segmented into different tissue types and spatially normalized to the MNI template as implemented in the CAT12 toolbox.

Brain volumes, including volumes of hippocampus and middle-inferior temporal gyrus, were extracted from the spatially normalized gray matter tissue segments using the anatomical labels provided in the Hammers atlas (Hammers et al., 2003). We localized the cholinergic space of the basal forebrain based on a cytoarchitectonic map of BF cholinergic nuclei in MNI space, derived from combined histology and MRI of a post-mortem brain, as described previously (Kilimann et al., 2014). All volumes were scaled to each individual's total intracranial volume, calculated as the sum of the total gray matter, white matter, and cerebrospinal fluid tissue segments.

2.7. Statistics

Group comparisons of demographic and volumetric data were performed using *Jeffreys' Amazing Statistics Program* (JASP Version 0.16.3), available at jasp-stats.org. We compared age, interval between MRI and death, as well as regional brain volumes between groups using Bayesian ANCOVA. Volumetric analyses were controlled for age, sex, and diagnosis, as well as the interval between MRI and death. Sex, diagnosis, and neuropathology ratings were compared between groups using contingency tables. We report the Bayes Factor (BF_{10}) quantifying evidence against the null hypotheses (Wagenmakers et al., 2018). For volumetric analysis where the Bayes factor for the alternative model (BF_{10}) indicated at least a moderate level of evidence in favor of a difference between groups, i.e. $BF_{10} > 3$, we used post hoc tests for group differences with prior odds corrected for multiple testing (Westfall et al., 1997) using JASP's default setting.

We used voxel-based receiver operating characteristics (ROC) analysis in the training sample from ADNI to identify brain regions that best discriminate pure AD cases from pure TDP-43 cases. The area under the ROC curve (AUC) at each voxel was calculated using the library "precrec" in R version 4.2.2 (2022−10−31) accessed through RStudio. We thresholded scans to retain only voxels with an AUC above 80%. We identified spatial clusters from the identified voxels using an algorithm proposed at (https://stackoverflow.com/questions/47093861/spatial-clustering-3d-array-with-neighbourhood-strategy-in-r) and kept only clusters containing at least 100 neighboring voxels. Cluster centroids were determined as the medoids[2] (Kaufman and Rousseeuw, 1987) of each single cluster using command "pam" in the R library "cluster". The clusters and their medoids were overlaid on an MRI template in MNI space and MNI coordinates were derived from the anatomical space coordinates in FSLeyes version 0.31.2 (FMRIB Centre, Oxford, UK).

Group separation between pure AD and pure TDP-43 cases in the NACC test sample was determined using ROC curve analysis with the averaged volume of the previously identified clusters as well as using hippocampal and middle-inferior temporal gyrus volumes and their ratio as previously described in the literature (Botha et al., 2018; Teipel

[2] Medoids are representatives of clusters "which minimize the average dissimilarity of all objects of the data set to the nearest medoid." Kaufman, L., Rousseeuw, P. J., Clustering by means of medoids. In: Y. Dodge, (Ed.), Statistical Data Analysis based on the L1 Norm. North-Holland, Amsterdam, 1987, pp. 405–416.

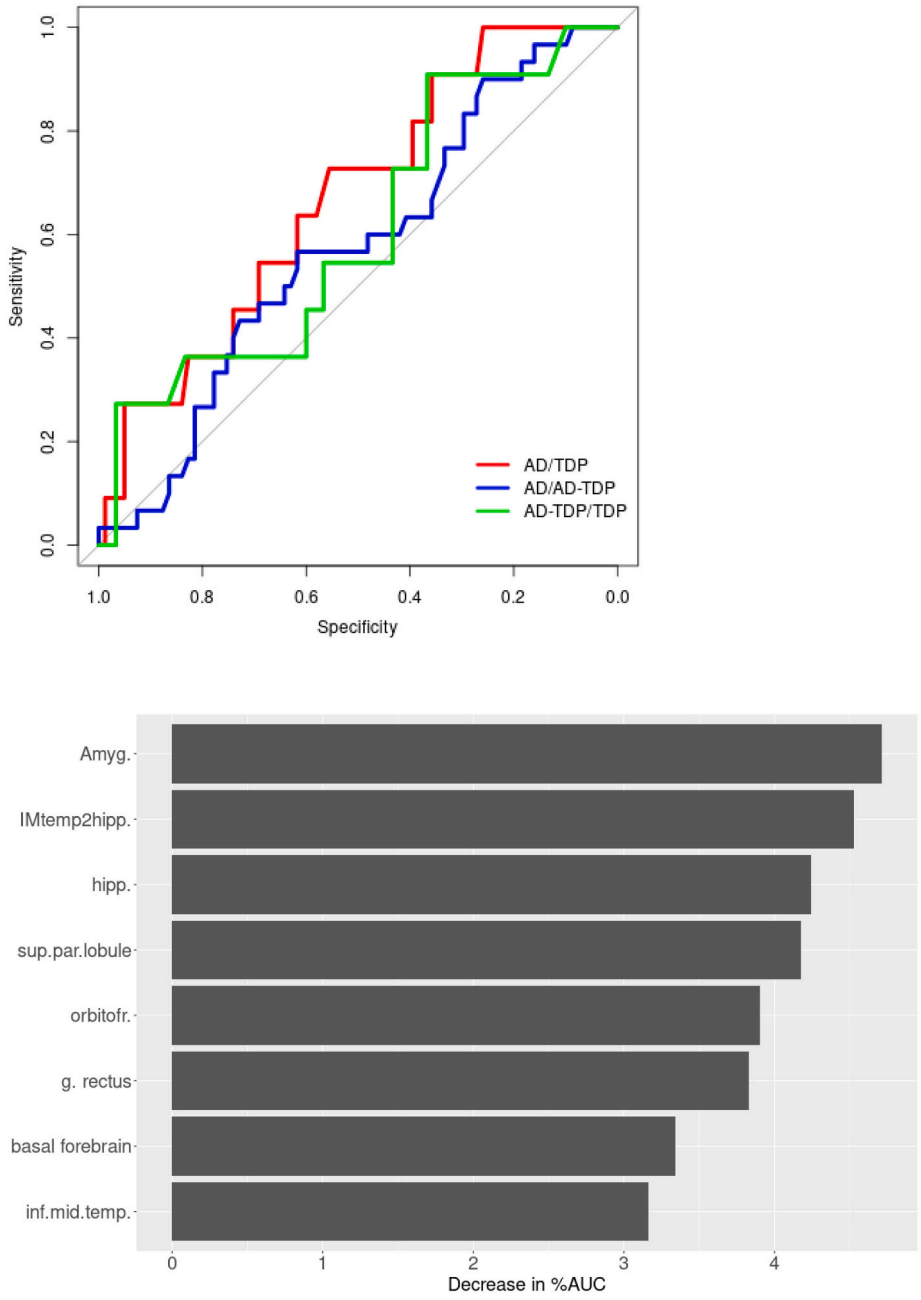

Fig. 4. Separation between pure AD, pure TDP-43 and mixed AD/TDP-43 in the NACC cohort.
a: Exemplary ROC curves.
b: Contribution of volumes to group separation – decrease in % of AUC.

et al., 2022). ROC curve analyses used the library "ROCnReg" in R version 4.2.2 (2022-10-31).

In a complementary data-driven separation between the three groups of pure AD, pure TDP-43, and mixed AD/TDP-43 in the ADNI and the NACC samples, we first examined the distribution of hippocampal volume, basal forebrain volume, and middle-inferior temporal gyrus to hippocampal ratio. The corresponding figure indicated that a linear discrimination approach was not useful for distinguishing the three groups (Fig. 1). Therefore, we used a random forest approach that allows for non-linear separation of groups (James et al., 2013) (pages 303–335). We conducted this analysis in two steps. First, we identified the accuracy gain or decrease that was associated with each of many regions of the 'Hammers' maximum probability structural atlas (Hammers et al., 2003) (specifically gray matter volumes of amygdala, hippocampus, and cingulate gyrus, as well as all 'Hammers' atlas cortical regions, excluding precentral and postcentral gyrus). We then selected those regions that showed a maximum accuracy gain for the separation of the three groups and fed these regions into a random forest analysis with a training and test set approach. Due to the unbalanced distribution of groups, we used the area under the ROC curve in the test data as the accuracy measure. We used a random sample of 50% of the cases per cohort for training and the remaining sample for testing. Because we had to separate three classes we used the "multiclass.roc" command of the "pROC" package in R version 4.2.2 (2022-10-31). Multiclass AUC determines an average of all pairwise ROC curve comparisons between the three groups, i.e. AD vs. TDP-43, AD vs. AD/TDP-43, and AD/TDP-43 vs. TDP-43, as described in (Hand and Till, 2001). We used 100 bootstrapping iterations to repeat the random forest

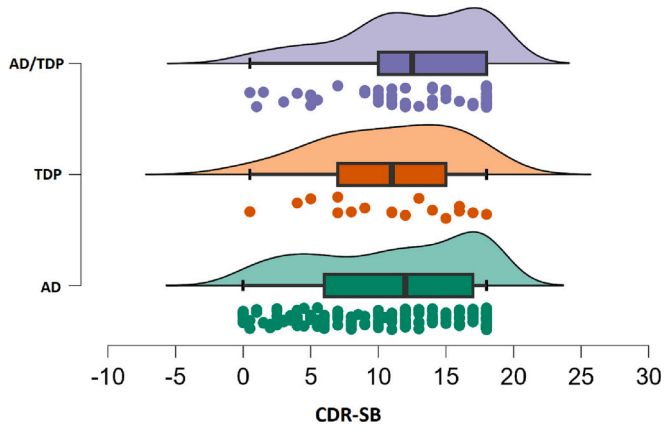

Fig. 5. Rainbow plot for CDR-SB by pathological group.

classifications over random samples of the training and test data to determine resulting mean and standard deviations of AUC values for the group separation.

3. Results

3.1. Demographics

The ADNI sample contained 11 cases with a TDP-43 sum score ≥ 2 and an ADNC score ≤ 1, labeled pure TDP-43 cases, 47 cases with a TDP-43 score $= 0$ and an ADNC score ≥ 2, labeled pure AD cases, and 26 cases with an ADNC score ≥ 2 and TDP-43 sum score ≥ 2, labeled mixed AD/TDP-43 cases. These are one additional pure TDP-43 case and 14 additional pure AD cases compared to our previous analysis of the ADNI autopsy data; the group of mixed cases was not included in the previous analysis (Teipel et al., 2022). According to the same criteria, the NACC sample contained 17 pure TDP-43 cases, 170 pure AD cases, and 58 mixed AD/TDP-43 cases.

In both cohorts, TDP-43 cases were numerically older than pure AD cases with moderate evidence for a difference between the mixed and the pure AD cases from the NACC cohort. Distribution of last CDR global score and sex did not differ between groups. In the ADNI cohort, there was no conclusive evidence for a difference in basal forebrain neuron numbers between groups. As expected, in both cohorts there was very strong to extreme evidence in favor of a higher proportion of hippocampal sclerosis in cases with TDP-43 pathology, but groups did not differ with respect to Lewy body pathology. In the NACC, but not the ADNI cohort, cases with TDP-43 pathology had longer intervals between MRI scans and death, with most pronounced group differences between the pure AD and the mixed AD/TDP-43 group. Detailed demographics are displayed in Tables 1 and 2.

3.2. Volumetric analyses

Analyses were controlled for age at death, sex, last CDR score, and interval between MRI scan and death. In the ADNI data, we found moderate evidence against a group effect on basal forebrain volume ($BF_{10} = 0.229$) or middle-inferior temporal gyrus volume ($BF_{10} = 0.190$). The evidence against an effect on basal forebrain volume was preserved when adding the degree of Lewy body pathology to the null model ($BF_{10} = 0.209$). We found inconclusive evidence for a group effect of lower hippocampus volume in pure TDP-43 compared to AD ($BF_{10} = 2.097$). In contrast, we found strong evidence for a group effect of higher middle-inferior temporal to hippocampus volume ratio in pure TDP-43 compared to pure AD ($BF_{10} = 24.4$).

In the NACC data, we found moderate evidence for the absence of a difference in basal forebrain and middle-inferior temporal gyrus volumes ($BF_{10} = 0.300$ and 0.115, respectively). When adding Lewy body

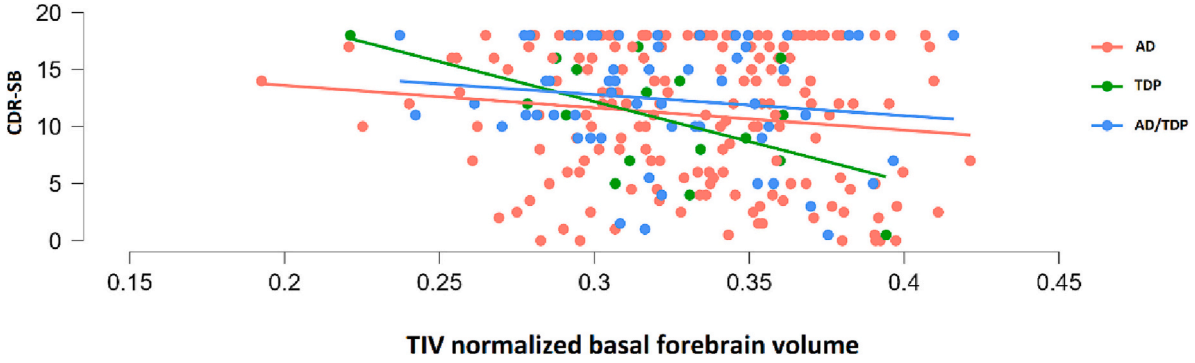

Fig. 6. Scatter plot of CDR-SB and basal forebrain volume by pathological group.

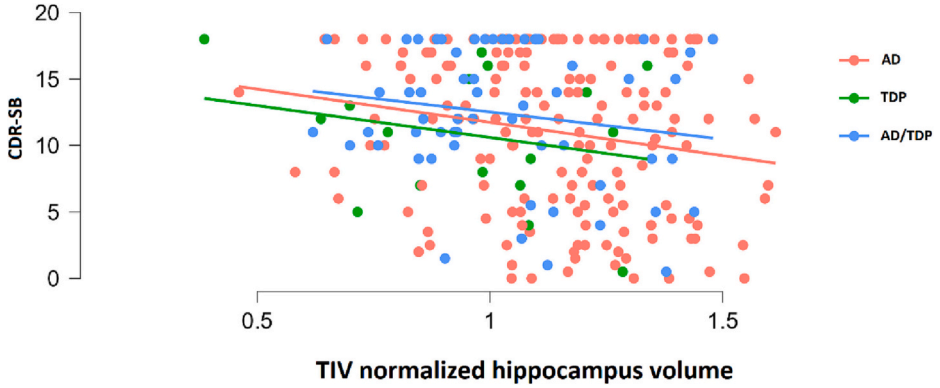

Fig. 7. Scatter plot of CDR-SB and hippocampus volume by pathological group.

pathology to the null model, results remained essentially unchanged. By contrast, we found very strong evidence for lower hippocampus volume and higher middle-inferior temporal gyrus to hippocampus ratio in pure TDP-43 cases compared to pure AD (BF_{10} = 98.238 and 275.03, respectively). These effects where preserved when adding hippocampal sclerosis to the null model (hippocampus volume: BF_{10} = 34.29; middle-inferior temporal gyrus to hippocampus ratio: 106.05).

Results of post-hoc tests for hippocampus volume and middle-inferior temporal gyrus to hippocampus ratio between the three groups are shown in Tables 3 and 4 for the ADNI and NACC cohorts, respectively. Boxplots of volumes according to AD/TDP-43 status are shown in Fig. 2. Numerically, average hippocampus volume and middle-inferior temporal gyrus to hippocampus ratio in the mixed AD/TDP-43 cases lay in between the pure AD and the pure TDP-43 cases. In the ADNI cohort there was only inclonclusive evidence for lower hippocampal volume in mixed AD/TDP-43 cases compared to pure AD, but moderate evidence for a higher middle-inferior temporal gyrus to hippocampus ratio. In the NACC cohort, there was strong evidence for both lower hippocampus volume and higher middle-inferior temporal gyrus to hippocampus ratio in the mixed AD/TDP-43 cases compared to pure AD. The level of evidence for hippocampal volume as a function of the number of cases in the ADNI and NACC cohorts, respectively, is shown in Supplementary Figs. 1 and 2.

3.3. Group separation between pure TDP-43 and pure AD cases based on brain AUC maps

In the ADNI data we found nine clusters of at least 100 neighboring voxels separating pure AD and pure TDP-43 cases with an AUC above 80%. The corresponding centroid coordinates in MNI space and the anatomical regions covered by these clusters are reported in Table 5 and illustrated in Fig. 3. Volumes were larger in pure TDP-43 cases than in pure AD cases in middle-inferior temporal gyrus, fusiform gyrus and middle occipital gyrus. There were no clusters with larger volumes in pure AD than in pure TDP-43 reaching an AUC of 80% or higher. The gray matter volumes of the combined clusters reached an AUC of 93% in the training data for discriminating pure AD and TDP-43 cases.

We transferred these clusters to the NACC data. When we used the cluster values derived from the ADNI data, we reached an AUC of 61.1% for discriminating pure AD and pure TDP-43 cases. However, when using the ratio of the cluster to the hippocampal volume, the AUC was increased to 75%. For comparison, the a priori ratio of middle-inferior temporal gyrus to hippocampus volume (Teipel et al., 2022) reached an AUC of 77%.

With a voxel-wise AUC analysis applied to the NACC data we found a relatively small cluster in the inferior parietal lobe reaching an AUC > 70% for separating pure AD and TDP-43 cases. This cluster overlapped with the clusters found for the ADNI sample but was much more spatially restricted (Fig. 3). We found no voxel at an AUC > 80% for the NACC data.

3.4. Data driven random forest analysis for separating pure AD, pure TDP-43, and mixed AD/TDP-43 cases

Using an optimized non-linear random forest approach, where the primary selection of the regions was based on the training sample, the mean multiclass AUC over 100 iterations was only 0.61 (SD 0.07) in the test sample from the ANDI cohort and 0.63 (SD 0.04) in the test sample from the NACC cohort. An exemplary plot of the pairwise ROC curves for the ADNI cohort is shown in Supplementary Fig. 3a, for the NACC cohort in Fig. 4a. In the ADNI cohort, the most important separating regions were the middle-inferior temporal gyrus to hippocampus ratio, the posterior temporal lobe, and the cuneus, according to the percentage change in AUC averaged across the 100 iterations (Supplementary Fig. 3b). In the NACC sample, the most important separating regions were the amygdala, the middle-inferior temporal gyrus to hippocampus ratio, and the hippocampus (Fig. 4b).

3.5. Association of cognitive scores with pathological groups and volumes

We found moderate evidence (BF_{10} = 3.82) for an effect of pathological group (AD, TDP-43, mixed AD/TDP-43) on CDR-SB score in a Bayesian ANCOVA, controlling for age at neuropsychological testing, sex, and distance between testing and death. CDR-SB values were highest for the mixed AD/TDP-43 cases, intermediate for the AD cases, and lowest for the TDP-43 cases (see Fig. 5). For MMSE score, logical memory, digit span forward and TMTB-A we found moderate to anecdotal evidence (BF_{10} < 0.54) against an association with pathology group, based on a relatively small number of cases.

We found strong evidence for an effect of basal forebrain volume (BF_{10} = 15.2), and very strong evidence for an effect of hippocampus volume (BF_{10} = 536.9) on CDR-SB with smaller CDR-SB scores (i.e. better function) with larger volumes, after controlling for pathological group, age at testing, sex and distance between neuropsychological testing and death. The effects were similar within each pathological group for both basal forebrain and hippocampus, see Figs. 6 and 7.

4. Discussion

Here, we studied differences in basal forebrain atrophy as well as brain wide volumetric signatures in patients with pure AD pathology, pure TDP-43 pathology, and in mixed AD/TDP-43 cases. Confirming and extending previous evidence from the ANDI autopsy sample (Teipel et al., 2022), we found evidence in favor of no group difference in basal forebrain volumes between the three groups, both in the ADNI and the NACC autopsy samples. In addition, we found more pronounced hippocampus atrophy in mixed AD/TDP-43 and in pure TDP-43 cases than in pure AD cases (Josephs et al., 2008) in the NACC sample, but not an additive effect of mixed AD/TDP-43 pathology compared with TDP-43 pathology alone. A volumetric marker of the middle-inferior temporal gyrus to hippocampus ratio identified from previous studies (Botha et al., 2018; Grothe et al., 2022; Teipel et al., 2022) reached an AUC of about 77% in the NACC sample. When identifying a volumetric marker directly from the data using voxel-based AUC analysis, we found a regional pattern of preserved inferior and lateral temporo-occipital brain volume in TDP-43 that separated groups with >90% accuracy in the ADNI training data but reached poor accuracy in the NACC test sample. Only in combination with hippocampus volume did this volumetric signature reach an AUC of 75% similar to the a priori middle-inferior temporal gyrus to hippocampus ratio. Using an optimized data-driven random forest approach, group separation between AD, TDP-43, and the mixed AD/TDP-43 group did not exceed a multiclass AUC of 61% in the ADNI data and 63% in the NACC data, which was above chance level but not sufficient for diagnostic use.

Our findings of pronounced hippocampus atrophy in TDP-43 cases in the NACC cohort replicate well-established findings from previous studies (Bejanin et al., 2019; Josephs et al., 2017; Josephs et al., 2008). In the ADNI cohort, hippocampus volume was numerically smaller in the TDP-43 cases, but the sequential analysis suggested (Supplementary Fig. 1) that the number of cases was not sufficient to reach a conclusive level of evidence. A previous study had suggested that effects of TDP-43 on hippocampus atrophy may be independent of other pathologies, including AD type tau pathology (Buciuc et al., 2020). Therefore, we had expected that a combination of both AD and TDP-43 pathologies may lead to more pronounced atrophy of the hippocampus than TDP-43 pathology alone. Contrary to this expectation, we found no evidence for a difference between the TDP-43 and the mixed AD/TDP-43 groups in hippocampus atrophy in either cohort.

A similar degree of basal forebrain atrophy in both TDP-43 and AD/TDP-43 cases compared with pure AD cases suggests a similar cholinergic deficit in limbic TDP-43 even independently from AD pathology. This differs from the TDP-43 pathology associated with frontotemporal

lobar degeneration (FTLD) or primary progressive aphasias (PPA). Here, previous autopsy studies reported no loss of cholinergic basal forebrain neurons compared with control brains in FTLD or PPA cases without concomitant AD pathology (Dunlop et al., 2022; Schaeverbeke et al., 2022), reviewed in (Geula et al., 2021). Of note, basal forebrain atrophy and neuronal loss are not identical markers of basal forebrain pathology. In early stages of AD, a previous study suggested that the basal forebrain exhibits neurofibrillary tangle accumulation and dystrophic cell shrinkage of cholinergic neurons, but not major neuronal loss (Mufson et al., 2003). In the ADNI autopsy sample we identified only five pure TDP-43 cases with reported extent of basal forebrain neuron loss (Teipel et al., 2020) leading to inconclusive evidence for or against an effect. In the NACC autopsy sample, basal forebrain neuron numbers have not been reported. Still, our consistent findings in the ADNI and NACC samples suggest that limbic TDP-43, different to TDP-43 pathology in FTLD-TDP and ALS, is associated with basal forebrain degeneration, even when accounting for Lewy body pathology. This supports a clinical trial of the effects of cholinergic treatment in amnestic dementia due to limbic TDP-43.

Currently, we do not have molecular in vivo markers of TDP-43 pathology available. CSF markers of TDP-43 are being developed but are not yet ready for clinical use or case selection in clinical trials (Scialo et al., 2020). Therefore, we assessed the usefulness of widely accessible MRI volumetric markers to discriminate TDP-43 from AD cases. We found very high discrimination of pure AD and pure TDP-43 cases in the ADNI autopsy sample based on a regional pattern of preserved brain volume in lateral temporal, fusiform, occipital, and middle frontal gyrus derived from voxel based ROC curve analysis. However, this pattern only provided poor separation when transferred to the NACC sample. Group discrimination accuracy was higher with about 75% AUC when additionally considering hippocampus volume. This level of accuracy was similar to the accuracy provided by the previously proposed ratio of middle-inferior temporal gyrus to hippocampus volume (Botha et al., 2018; Grothe et al., 2022; Teipel et al., 2022) with an AUC of about 77%. This level of accuracy would be sufficient for group-level analysis, but not for single case identification. Of note, this accuracy is based on the test sample, as training was performed in the ADNI sample or the regions had been derived from the literature.

In contrast, separation between the three groups of AD, TDP-43, and mixed AD/TDP-43 using random forest analysis reached only a cross-validated multiclass AUC between 61% to 63%, which was above chance level, but not sufficient even for group level analyses. This low group separation may be expected considering that it is difficult to separate mixed pathology from single pathology cases unless the mixed pathology results in a synergistic effect on brain atrophy that exceeds the effect of either pathology alone.

The association of pathological group with CDR-SB scores in the NACC sample agree with the observation that pure limbic TDP-43 cases have a more benign course of cognitive decline than AD cases (Nelson et al., 2019) and an additive pathology of TDP-43 and AD in the mixed group, as previously suggested (Josephs et al., 2017). The number of cases particularly in the TDP-43 group was very small when we considered associations of pathological group with cognitive scores, such as MMSE, logical memory, and TMTB-A. This rendered the results uninformative when comparing the TDP-43 cases with the other groups.

We must point out some limitations of our study: First, the pathology data were based on retrospective data repositories; the authors did not have access to the autopsy specimens themselves. ADNI and NACC follow the same standard operating procedures for neuropathologic examinations. The ADNI has a single central autopsy core, whereas the NACC autopsy data come from different neuropathology laboratories and are thus subject to additional variation. In addition, MRI scans are more heterogeneous between NACC sites than between ADNI sites. However, despite these heterogeneities, the results were highly consistent between the ADNI and NACC samples. This highlights the robustness of our results. Despite the use of the relatively large NACC autopsy sample, the number of pure TDP-43 cases remained small. This number allowed us to assess additional effects of Lewy body pathology and hippocampal sclerosis but precluded finer classification into additional subtypes. Bayesian analysis helped us to determine whether the effects were robust despite the small sample size by performing sequential analyses.

In summary, we wanted to test our previous finding (Teipel et al., 2022) of basal forebrain cholinergic atrophy in cases with limbic TDP-43 pathology. Evidence is accumulating that a relevant proportion of clinical research findings cannot be replicated (Anderson et al., 2016; Gilbert et al., 2016; Goodman and Greenland, 2007; Ioannidis, 2007; Open Science, 2015), underscoring the importance of replication studies (Baker, 2016). Our previous work was based on a small number of cases that allowed us to hypothesize, but not confirm, basal forebrain atrophy in limbic TDP-43. Here, we used an independent cohort to test this hypothesis. In addition, we also confirmed the utility of the ratio of middle-inferior temporal gyrus to hippocampus volume in discriminating TDP-43 and AD cases with similar accuracy in the ADNI and the NACC cohorts. A novel aspect is that a finer-grained atrophy pattern that we identified data-driven in the ADNI cohort was not transferable to the NACC data unless we added hippocampus volume. This may be related to the greater inhomogeneity of the NACC MRI data compared with the ADNI MRI data, among other factors. We also added a group of mixed AD/TDP-43 cases, and group separation based on MRI volumetric markers across the three groups was relatively poor. Our findings encourage investigating the potential impact of cholinergic treatment in amnestic dementia cases with evidence of TDP-43 pathology. However, in-vivo identification of these individuals is currently limited by the lack of in vivo biomarkers for TDP-43 pathology. A distinct MRI-based pattern of brain atrophy, with relatively preserved middle-inferior temporal lobe and more reduced hippocampal volume, may serve as a surrogate marker to enrich samples in clinical trials for the presence of TDP-43 pathology.

CRediT authorship contribution statement

Stefan Teipel: Conceptualization, Methodology, Data curation, Formal analysis, Writing – original draft. **Michel J. Grothe:** Conceptualization, Methodology, Writing – review & editing.

Declaration of Competing Interest

ST participated in scientific advisory boards of Roche Pharma AG, Biogen, Grifols, and MSD, and is member of the Independent Data Safety and Monitoring Board of the study ENVISION (Biogen). MG reports no conflicts of interest.

Data availability

Data will be made available on request.

Acknowledgments

MJG is supported by the “Miguel Servet” Program [CP19/00031] and a research grant [PI20/00613] of the Instituto de Salud Carlos III-Fondo Europeo de Desarrollo Regional (ISCIII-FEDER), Spain. Part of the data collection and sharing for this project was funded by the Alzheimer’s Disease Neuroimaging Initiative (ADNI) (National Institutes of Health Grant U01 AG024904) and DOD ADNI (Department of Defense award number W81XWH-12-2-0012). ADNI is funded by the National Institute on Aging, the National Institute of Biomedical Imaging and Bioengineering, and through generous contributions from the following: Alzheimer’s Association; Alzheimer’s Drug Discovery Foundation; Araclon Biotech; BioClinica, Inc.; Biogen Idec Inc.; Bristol-Myers Squibb Company; Eisai Inc.; Elan Pharmaceuticals, Inc.; Eli Lilly and Company; EuroImmun; F. Hoffmann-La Roche Ltd. and its affiliated company

Genentech, Inc.; Fujirebio; GE Healthcare; IXICO Ltd.; Janssen Alzheimer Immunotherapy Research & Development, LLC.; Johnson & Johnson Pharmaceutical Research & Development LLC.; Medpace, Inc.; Merck & Co., Inc.; Meso Scale Diagnostics, LLC.; NeuroRx Research; Neurotrack Technologies; Novartis Pharmaceuticals Corporation; Pfizer Inc.; Piramal Imaging; Servier; Synarc Inc.; and Takeda Pharmaceutical Company. The Canadian Institutes of Health Research is providing funds to support ADNI clinical sites in Canada. Private sector contributions are facilitated by the Foundation for the National Institutes of Health (www.fnih.org). The grantee organization is the Northern California Institute for Research and Education, and the study is coordinated by the Alzheimer's Disease Cooperative Study at the University of California, San Diego. ADNI data are disseminated by the Laboratory for Neuro Imaging at the University of Southern California.

The NACC database is funded by NIA/NIH Grant U24 AG072122. NACC data are contributed by the NIA-funded ADRCs: P30 AG062429 (PI James Brewer, MD, PhD), P30 AG066468 (PI Oscar Lopez, MD), P30 AG062421 (PI Bradley Hyman, MD, PhD), P30 AG066509 (PI Thomas Grabowski, MD), P30 AG066514 (PI Mary Sano, PhD), P30 AG066530 (PI Helena Chui, MD), P30 AG066507 (PI Marilyn Albert, PhD), P30 AG066444 (PI John Morris, MD), P30 AG066518 (PI Jeffrey Kaye, MD), P30 AG066512 (PI Thomas Wisniewski, MD), P30 AG066462 (PI Scott Small, MD), P30 AG072979 (PI David Wolk, MD), P30 AG072972 (PI Charles DeCarli, MD), P30 AG072976 (PI Andrew Saykin, PsyD), P30 AG072975 (PI David Bennett, MD), P30 AG072978 (PI Neil Kowall, MD), P30 AG072977 (PI Robert Vassar, PhD), P30 AG066519 (PI Frank LaFerla, PhD), P30 AG062677 (PI Ronald Petersen, MD, PhD), P30 AG079280 (PI Eric Reiman, MD), P30 AG062422 (PI Gil Rabinovici, MD), P30 AG066511 (PI Allan Levey, MD, PhD), P30 AG072946 (PI Linda Van Eldik, PhD), P30 AG062715 (PI Sanjay Asthana, MD, FRCP), P30 AG072973 (PI Russell Swerdlow, MD), P30 AG066506 (PI Todd Golde, MD, PhD), P30 AG066508 (PI Stephen Strittmatter, MD, PhD), P30 AG066515 (PI Victor Henderson, MD, MS), P30 AG072947 (PI Suzanne Craft, PhD), P30 AG072931 (PI Henry Paulson, MD, PhD), P30 AG066546 (PI Sudha Seshadri, MD), P20 AG068024 (PI Erik Roberson, MD, PhD), P20 AG068053 (PI Justin Miller, PhD), P20 AG068077 (PI Gary Rosenberg, MD), P20 AG068082 (PI Angela Jefferson, PhD), P30 AG072958 (PI Heather Whitson, MD), P30 AG072959 (PI James Leverenz, MD).

Appendix A. Supplementary data

Supplementary data to this article can be found online at https://doi.org/10.1016/j.nbd.2023.106070.

References

Anderson, C.J., et al., 2016. Response to comment on "estimating the reproducibility of psychological science". Science. 351, 1037.
Baker, M., 2016. 1,500 scientists lift the lid on reproducibility. Nature. 533, 452–454.
Bejanin, A., et al., 2019. Antemortem volume loss mirrors TDP-43 staging in older adults with non-frontotemporal lobar degeneration. Brain. 142, 3621–3635.
Besser, L.M., et al., 2018. The revised National Alzheimer's coordinating Center's neuropathology form-available data and new analyses. J. Neuropathol. Exp. Neurol. 77, 717–726.
Botha, H., et al., 2018. FDG-PET in tau-negative amnestic dementia resembles that of autopsy-proven hippocampal sclerosis. Brain. 141, 1201–1217.
Buciuc, M., et al., 2020. Effect modifiers of TDP-43-associated hippocampal atrophy rates in patients with Alzheimer's disease neuropathological changes. J. Alzheimers Dis. 73, 1511–1523.
Dunlop, S.R., et al., 2022. Resistance of basal forebrain cholinergic neurons to TDP-43 proteinopathy in primary progressive aphasia. J. Neuropathol. Exp. Neurol. 81, 910–919.
Franklin, E.E., et al., 2015. Brain collection, standardized neuropathologic assessment, and comorbidity in Alzheimer's disease neuroimaging initiative 2 participants. Alzheimers Dement. 11, 815–822.
Geula, C., et al., 2021. Basal forebrain cholinergic system in the dementias: vulnerability, resilience, and resistance. J. Neurochem. 158, 1394–1411.
Gilbert, D.T., et al., 2016. Comment on "estimating the reproducibility of psychological science". Science. 351, 1037.
Goodman, S., Greenland, S., 2007. Why most published research findings are false: problems in the analysis. PLoS Med. 4, e168.
Grothe, M.J., et al., 2022. Differential diagnosis of amnestic dementia patients based on an FDG-PET signature of autopsy-confirmed LATE-NC. Alzheimers Dement. 1–11. https://doi.org/10.1002/alz.127632022.
Hammers, A., et al., 2003. Three-dimensional maximum probability atlas of the human brain, with particular reference to the temporal lobe. Hum. Brain Mapp. 19, 224–247.
Hand, D.J., Till, R.J., 2001. A simple generalisation of the area under the ROC curve for multiple class classification problems. Mach. Learn. 45, 171–186.
Ioannidis, J.P., 2007. Why most published research findings are false: author's reply to Goodman and Greenland. PLoS Med. 4, e215.
James, G.A., et al., 2013. An Introduction to Statistical Learning with Applications in R. Springer, New York.
Josephs, K.A., et al., 2008. Abnormal TDP-43 immunoreactivity in AD modifies clinicopathologic and radiologic phenotype. Neurology. 70, 1850–1857.
Josephs, K.A., et al., 2014. Staging TDP-43 pathology in Alzheimer's disease. Acta Neuropathol. 127, 441–450.
Josephs, K.A., et al., 2017. Rates of hippocampal atrophy and presence of post-mortem TDP-43 in patients with Alzheimer's disease: a longitudinal retrospective study. Lancet Neurol. 16, 917–924.
Katsumata, Y., et al., 2020. Distinct clinicopathologic clusters of persons with TDP-43 proteinopathy. Acta Neuropathol. 140, 659–674.
Kaufman, L., Rousseeuw, P.J., 1987. Clustering by means of medoids. In: Dodge, Y. (Ed.), Statistical Data Analysis Based on the L1 Norm. North-Holland, Amsterdam, pp. 405–416.
Kilimann, I., et al., 2014. Subregional basal forebrain atrophy in Alzheimer's disease: a multicenter study. J. Alzheimers Dis. 40, 687–700.
Montine, T.J., et al., 2012. National institute on aging-Alzheimer's association guidelines for the neuropathologic assessment of Alzheimer's disease: a practical approach. Acta Neuropathol. 123, 1–11.
Morris, J.C., 1993. The clinical dementia rating (CDR): current version and scoring rules. Neurology. 43, 2412–2414.
Morris, J.C., et al., 2006. The uniform data set (UDS): clinical and cognitive variables and descriptive data from Alzheimer disease centers. Alzheimer Dis. Assoc. Disord. 20, 210–216.
Mufson, E.J., et al., 2003. Human cholinergic basal forebrain: chemoanatomy and neurologic dysfunction. J. Chem. Neuroanat. 26, 233–242.
Nelson, P.T., et al., 2019. Limbic-predominant age-related TDP-43 encephalopathy (LATE): consensus working group report. Brain. 142, 1503–1527.
Open Science, C., 2015. PSYCHOLOGY. Estimating the reproducibility of psychological science. Science. 349, aac4716.
Robinson, J.L., et al., 2018. Neurodegenerative disease concomitant proteinopathies are prevalent, age-related and APOE4-associated. Brain. 141, 2181–2193.
Schaeverbeke, J., et al., 2022. Neuronal loss of the nucleus basalis of Meynert in primary progressive aphasia is associated with Alzheimer's disease neuropathological changes. Alzheimers Dement. https://doi.org/10.1002/alz.12794.
Scialo, C., et al., 2020. TDP-43 real-time quaking induced conversion reaction optimization and detection of seeding activity in CSF of amyotrophic lateral sclerosis and frontotemporal dementia patients. Brain Commun. 2, fcaa142.
Talairach, J., Tournoux, P., 1988. Co-Planar Stereotaxic Atlas of the Human Brain. Thieme, New York.
Teipel, S.J., et al., 2020. Neuropathologic features associated with basal forebrain atrophy in Alzheimer disease. Neurology. 95, e1301–e1311.
Teipel, S.J., et al., 2022. Antemortem basal forebrain atrophy in pure limbic TAR DNA-binding protein 43 pathology compared with pure Alzheimer pathology. Eur. J. Neurol. 29, 1394–1401.
Wagenmakers, E.J., et al., 2018. Bayesian inference for psychology. Part I: theoretical advantages and practical ramifications. Psychon. Bull. Rev. 25, 35–57.
Weintraub, S., et al., 2009. The Alzheimer's disease Centers' uniform data set (UDS): the neuropsychologic test battery. Alzheimer Dis. Assoc. Disord. 23, 91–101.
Westfall, P.H., et al., 1997. A Bayesian perspective on the Bonferroni adjustment. Biometrika. 84, 419–427.